ACS APPLIED MATERIALS & INTERFACES

www.acsami.org

Research Article

Immobilizing Enzymes on Noble Metal Hydrogel Nanozymes with Synergistically Enhanced Peroxidase Activity for Ultrasensitive Immunoassays by Cascade Signal Amplification

Jiajia Huang,[#] Lei Jiao,[#] Weiqing Xu, Qie Fang, Hengjia Wang, Xiaoli Cai, Hongye Yan, Wenling Gu, and Chengzhou Zhu*

Cite This: *ACS Appl. Mater. Interfaces* 2021, 13, 33383−33391

Read Online

ACCESS | Metrics & More | Article Recommendations | Supporting Information

ABSTRACT: Enzyme immobilization plays an essential role in solving the problems of the inherently fragile nature of enzymes. Although prominent stability and reuse of enzymes can be achieved by enzyme immobilization, their bioactivity and catalytic efficiency will be adversely affected. Herein, PdCu hydrogel nanozymes with a hierarchically porous structure were used to immobilize horseradish peroxidase (HRP) to obtain PdCu@HRP. In addition to the improvement of stability and reusability, PdCu@HRP displayed synergistically enhanced activities than native HRP and PdCu hydrogels. Not only the specific interactions between PdCu hydrogel nanozymes and enzymes but also the enrichment of substrates around enzymes by electrostatic adsorption of hydrogels was proposed to expound the enhanced catalytic activity. Accordingly, by taking advantage of the excellent catalytic performance of the PdCu@HRP and the glucose oxidase encapsulated in zeolitic imidazolate framework-8, colorimetric biosensing of the carcinoembryonic antigen via catalytic cascade reactions for achieving signal amplification was performed. The obtained biosensor enhanced the detection sensitivity by approximately 6.1-fold as compared to the conventional HRP-based enzyme-linked immunosorbent assay, demonstrating the promising potential in clinical diagnosis.

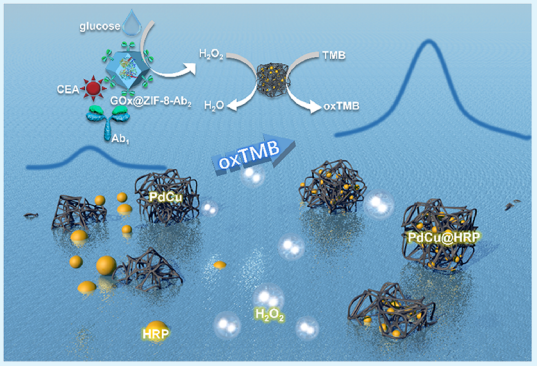

KEYWORDS: *noble metal hydrogels, enzyme immobilization, nanozymes, enzyme-linked immunosorbent assay, cascade signal amplification*

1. INTRODUCTION

Enzymes are a kind of highly efficient biological catalysts. However, the intrinsic limitations of natural enzymes, such as low stability and difficulty to recycle, have hampered their practical applications.[1−4] Enzyme immobilization as a critical technology for improving the stability and recyclability of the enzymes has aroused great interest in practical and commercial applications. Horseradish peroxidase (HRP), which is part of the superfamily of the heme-containing plant peroxidases,[5] has found widespread applications in disease diagnosis, sensing, pollutant degradation, and cancer treatment.[6−11] Some porous materials, such as mesoporous silica, metal−organic frameworks, and metallic oxides, have been proposed to serve as carriers for HRP immobilization.[12−18] The carriers with numerous pores and large specific surface areas play a critical role in preventing the agglomeration of enzymes and increasing the thermal/chemical stability and recyclability.[19−21] Yet, in many cases, the immobilized HRP can hardly maintain the high catalytic activity whether it is through covalent bonding, physical adsorption, or the encapsulation of enzymes in the nucleation process of carriers.[20,22,23] The denaturation and deactivation of the immobilized HRP are ascribed to the mass transfer limitations, unfavorable enzyme−carrier interactions, and conformational changes of the enzymes in the matrix.[20,23,24] Therefore, seeking more functional carriers to maintain or boost the catalytic activity of HRP is one of the high-priority research directions for its practical applications.

Noble metal hydrogels, emerging porous materials with superior catalytic activity, have received increasing attention in recent decades.[25−27] By accurately engineering the size, structure, and composition of the noble metal hydrogels, a precise control over their catalytic properties can be achieved.[28] Although the noble metal hydrogels have shown excellent catalytic activity,[29−31] their potential in immobilizing enzymes has rarely been explored. By taking advantage of the

Received: May 17, 2021
Accepted: June 30, 2021
Published: July 7, 2021

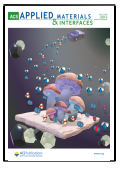

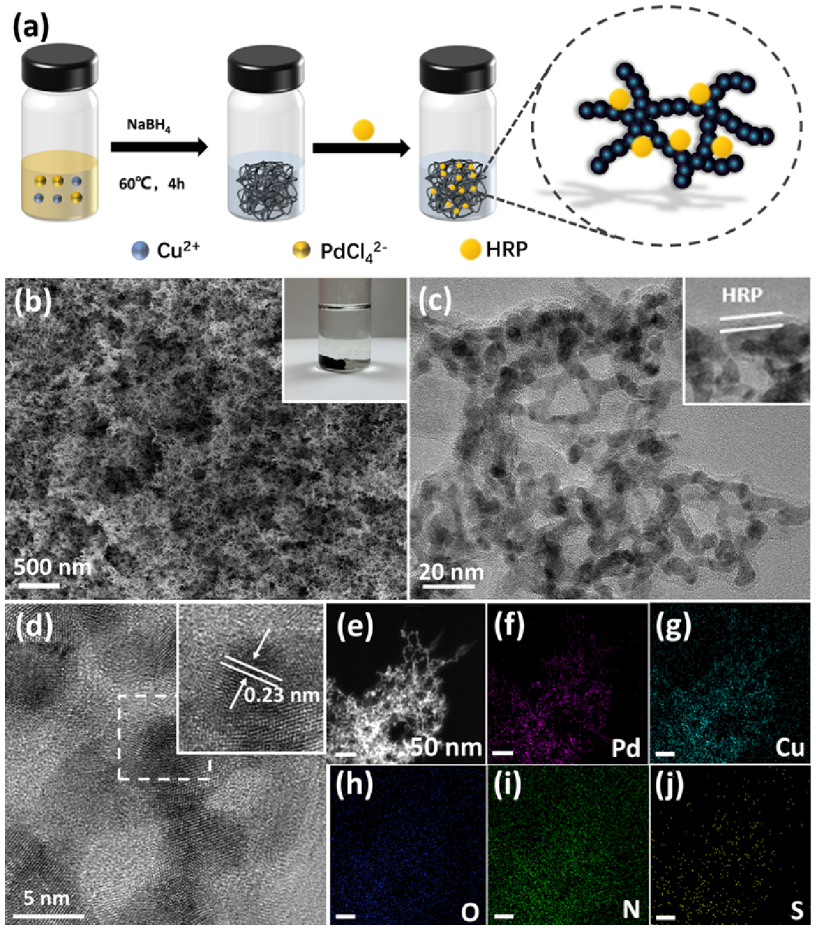

Figure 1. (a) Schematic illustration of the synthetic approach of PdCu@HRP. (b) SEM image of PdCu aerogels and a digital photo of PdCu hydrogels (inset). (c) TEM and (d) HRTEM images of the resulting PdCu@HRP. (e) HAADF−STEM image of PdCu@HRP and (f−j) corresponding elemental mapping images.

unique structures mentioned above, noble metal hydrogels hold great promise for loading enzymes. First, three-dimensional (3D) nanowire networks are beneficial to provide a high specific surface area and create a favorable microenvironment for loading enzymes.[32,33] The porous structure can also allow efficient mass transport and reduce diffusional resistance, enabling easier access to active sites of the enzymes by substrates.[28,29] Second, noble metals exhibit intrinsic affinity to proteins because noble metal ions can interact with surface functional groups on proteins.[34−36] This specific affinity also simplifies the procedures of enzyme immobilization without additional cross-linking agents. Finally, many noble metal nanomaterials and their alloy nanomaterials have shown promise as nanozymes and have been applied widely in the fields of biosensing and disease treatment.[2,37−39] Therefore, tuning noble metal hydrogel nanozymes is expected to efficiently immobilize enzymes and significantly boost their activity.

Herein, PdCu hydrogel nanozymes were synthesized and served as efficient carriers to load HRP. Their 3D porous nanowire networks with high porosity make them promising biocompatible supports for immobilizing HRP.[26] The affinity of Cu and Pd to proteins simplifies the procedures of enzyme immobilization without the addition of other cross-linking reagents.[34,35,40] As expected, the resulting PdCu@HRP exhibits enhanced tolerance to temperature and pH and realizes the reuse of HRP. Significantly, the peroxidase activity of PdCu@HRP is higher than those of free HRP, PdCu hydrogel nanozymes, and their mixtures, which indicates the existence of synergistic effects between PdCu hydrogel nanozymes and HRP. On the one hand, electron transfer between PdCu hydrogel nanozymes and HRP via coordination interaction leads to the activation of HRP, while the enzymelike activity of PdCu hydrogels is also favorable for the enhancement of the catalytic activity of PdCu@HRP. On the other hand, the negatively charged surface of PdCu can effectively attract positively charged substrates through electrostatic interactions, thereby achieving the enrichment of the substrates around the enzymes. As a proof-of-concept application, a cascade amplification strategy coupled with glucose oxidase (GOx) encapsulation in zeolitic imidazolate framework-8 (ZIF-8) was proposed for ultrasensitive colorimetric biosensing of the carcinoembryonic antigen (CEA). The resulting enzyme-linked immunosorbent assay (ELISA) showed 6.1-fold enhanced sensitivity than the commercial HRP-based conventional ELISA and was successfully explored for detecting biomarkers in human serum.

2. EXPERIMENTAL SECTION

2.1. Synthesis of PdCu Hydrogels and PdCu@HRP. Aqueous $NaBH_4$ (2 mL, 100 mM) was rapidly introduced into 32 mL of aqueous solution that contained H_2PdCl_4 (0.31 mM) and $CuCl_2$ (0.31 mM) under stirring at 60 °C for 1 min. The resulting solution was settled still at 60 °C for 4 h, and PdCu hydrogels were generated

https://doi.org/10.1021/acsami.1c09100
ACS Appl. Mater. Interfaces 2021, 13, 33383−33391

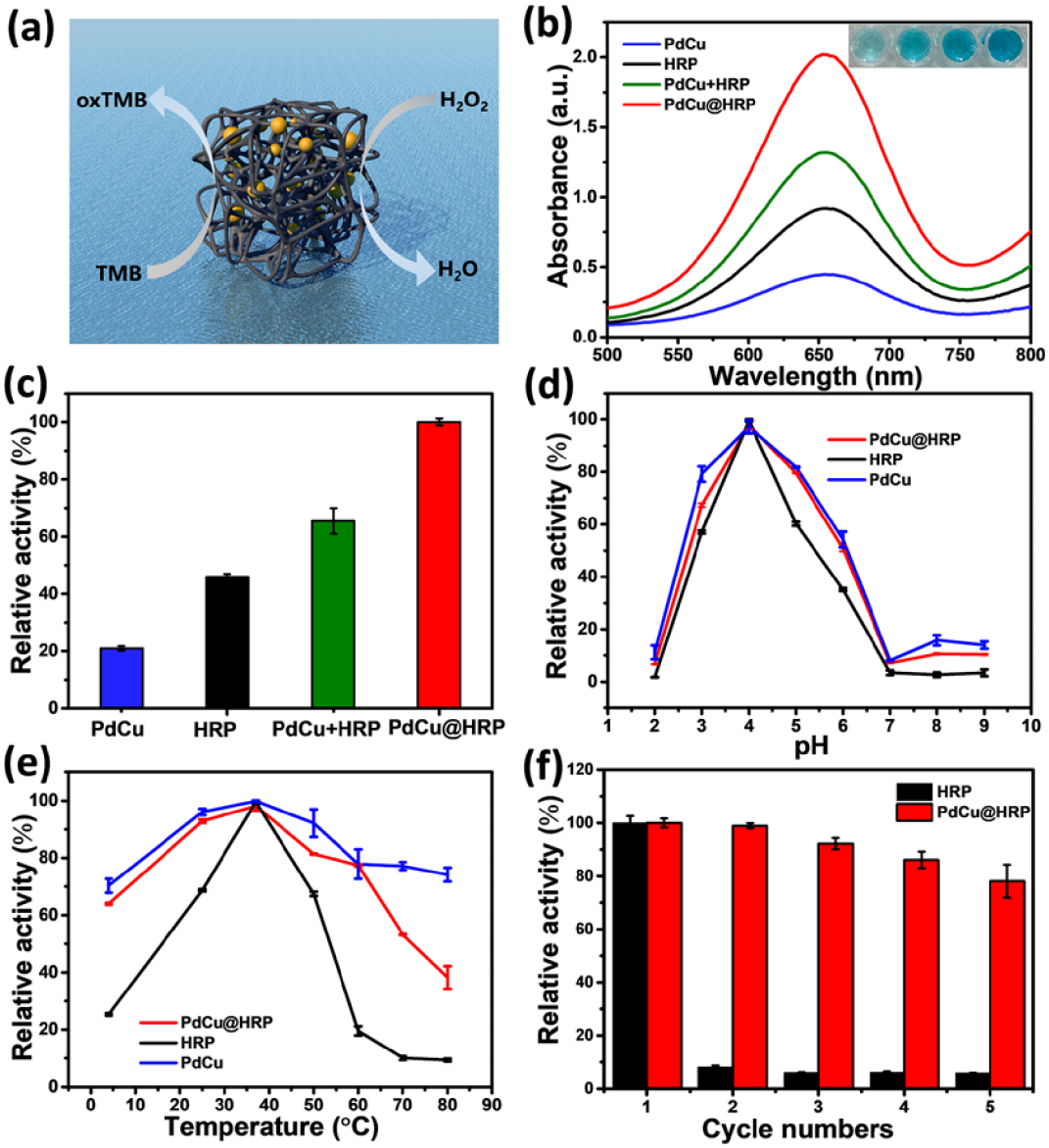

Figure 2. (a) Schematic illustration of the peroxidase-like activity of PdCu@HRP. (b) Absorbance spectra and digital photo (inset) of the HRP + TMB + H_2O_2, PdCu + TMB + H_2O_2, PdCu + HRP + TMB + H_2O_2, and PdCu@HRP + TMB + H_2O_2 in the sodium acetate (pH 4) buffer solution. (c) Relative activity of PdCu@HRP, PdCu + HRP, HRP, and PdCu. Effect of pH (d) and temperature (e) on PdCu@HRP, PdCu, and HRP activities. (f) Cycle numbers for PdCu@HRP and HRP.

at the bottom of the vial. After washing the PdCu hydrogels with water and dispersing in deionized water by ultrasound for 30 min, 2 mg of HRP was added into the resulting solution. PdCu@HRP was obtained after 2 h of stirring at room temperature and centrifuging to remove the free enzyme. The final washing solutions were collected to determine the protein concentration by the standard curve of the HRP concentration. The loading amount of HRP on the PdCu hydrogel was calculated based on the difference between the initial HRP amount added to the solution and the final HRP amount measured from the supernatant. Finally, the obtained PdCu@HRP was suspended in 1 mL of Milli-Q water for future use.

2.2. Measurement of Peroxidase-like Activity. The peroxidase-like activity was analyzed using TMB as a substrate. TMB (50 μL, 1 mM) was added to the mixture containing catalysts (10 μL, 0.01 mg mL^{-1}), H_2O_2 (100 μL, 100 mM), and sodium acetate buffer (150 μL, pH 4, 0.2 M) at 37 °C. The catalytic oxidation of TMB (oxTMB) can be quantitatively reflected by the absorbance at 652 nm recorded by a multimode reader. By changing the concentration of one substrate (H_2O_2 or TMB) and monitoring the absorption at 652 nm, the kinetic data were obtained. The kinetic parameters were obtained by the equation $V = V_{max} \times [S]/(K_m + [S])$, where K_m is the Michaelis constant, V is the initial velocity, V_{max} is the maximal velocity, and $[S]$ is the concentration of the substrate.

2.3. Procedure of the Immunoassays. First, 100 μL of Ab_1 (1 μg mL^{-1}) was pipetted into the 96-well microtiter plates and incubated at 4 °C overnight. After washing with PBS (0.01 M, pH 7.4) three times, 100 μL of blocking buffer (1% BSA in PBS) was spread onto each well for 0.5 h followed by rinsing three times with PBS. Afterward, 100 μL of CEA or human plasma sample (100-fold diluted with PBS) was added to the plates. After incubation for 1 h and washing steps, 100 μL of GOx@ZIF-8-Ab_2 (1 mg mL^{-1}) was added and incubated for 1 h at room temperature. Next, 150 μL of glucose (1 M) was introduced after washing, followed by 20 min of shaking at room temperature. Subsequently, 10 μL of PdCu@HRP (0.01 mg mL^{-1}), 100 μL of sodium acetate buffer (0.2 M, pH 4.0), and 50 μL of TMB (1 mM) were added to each well. The absorbance was recorded using a microplate reader after incubation for 20 min at 37 °C. The procedure of the HRP-based ELISA included using HRP-labeled Ab_2 to capture the CEA. After washing steps, 150 μL of sodium acetate buffer (0.2 M, pH 4.0), 100 μL of H_2O_2 (100 mM),

https://doi.org/10.1021/acsami.1c09100
ACS Appl. Mater. Interfaces 2021, 13, 33383−33391

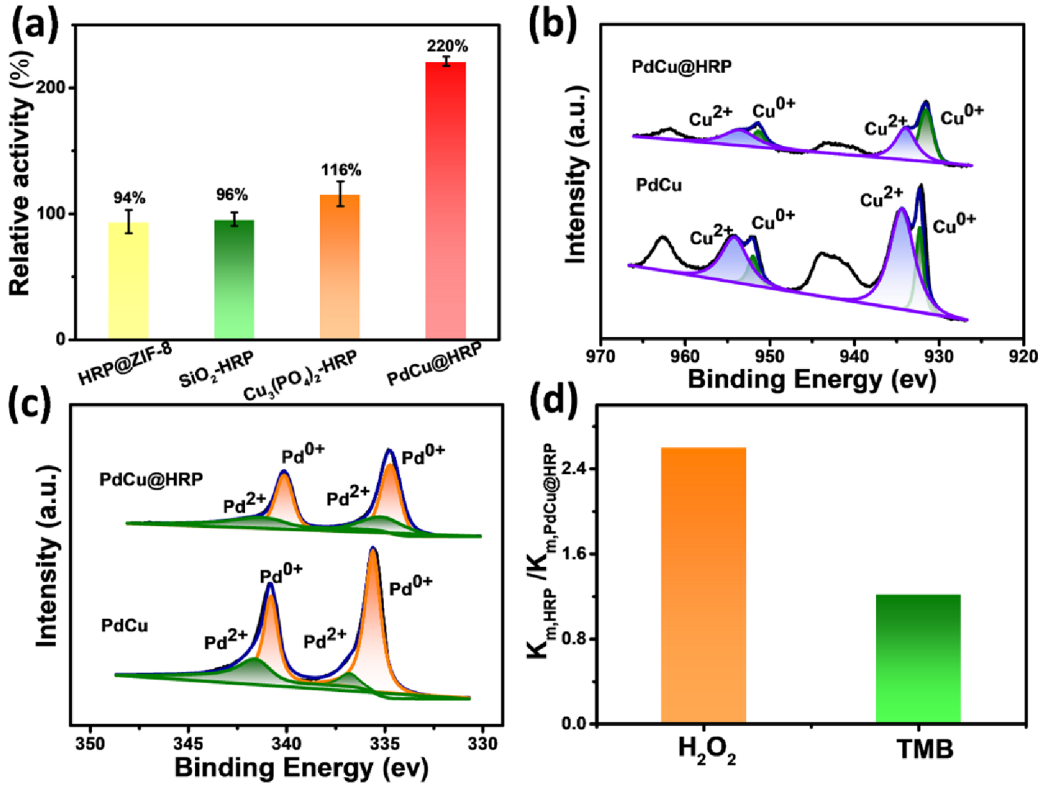

Figure 3. (a) Biocatalytic activity comparison of the representative enzyme−carrier systems, including HRP@ZIF-8, SiO_2−HRP, $Cu_3(PO_4)_2$−HRP, and PdCu@HRP (the free HRP activity was 100%). (b) XPS spectra of Cu 2p and (c) Pd 3d of the as-synthesized PdCu aerogels and PdCu@HRP. (d) Ratio of Michaelis constant K_m of PdCu@HRP and HRP for TMB or H_2O_2 substrates.

and 50 μL of TMB (1 mM) were added to each well. The absorbance intensities were recorded by the microplate reader after incubating for 20 min at 37 °C.

3. RESULTS AND DISCUSSION

3.1. Characterization of PdCu Hydrogels and PdCu@HRP. As shown in Figure 1a, one-step reduction using $NaBH_4$ was adopted to synthesize PdCu bimetallic hydrogels in an aqueous solution at 60 °C.[27] It was observed that metal precursors could be instantly reduced upon the introduction of reducing agents with the color changing from yellow to black. The solution was kept still for 4 h at 60 °C, and the jellylike PdCu hydrogels were generated at the bottom of the bottle (inset in Figure 1b). PdCu@HRP was obtained by directly adding HRP to the PdCu hydrogel solution. After 2 h of stirring at room temperature, HRP was immobilized on PdCu hydrogels because of the high affinity between proteins and PdCu hydrogels. PdCu aerogels were obtained by the supercritical CO_2 drying technique, and the porous structure made them have a relatively low density (Figure S1a). SEM was further performed to characterize the morphology of PdCu aerogels. As shown in Figure 1b, PdCu aerogels exhibited typical 3D network architectures with high specific surface area, being regarded as promising carriers for loading enzymes. To further characterize the fine structures of PdCu@HRP, TEM was employed. As shown in Figure 1c, the resulting PdCu@HRP consists of necklacelike interconnected nanowires, which maintain the structure of PdCu hydrogels (Figure S1b). Furthermore, careful observation of the nanostructure revealed that these nanowires are coated with transparent "water films" with a thickness of 2 nm, while the same phenomenon could not be observed in PdCu hydrogels (Figure S1c), which are inferred as the HRP layer (inset in Figure 1c). The high-resolution TEM (HRTEM) image in Figure 1d shows that the lattice spacing of PdCu@HRP is about 0.23 nm,[25] which is the same as that of PdCu hydrogels (Figure S1d). The elemental distribution was also investigated by high-angle annular dark-field scanning transmission electron microscopy (HAADF−STEM) mapping. Moreover, both metal elements (Pd and Cu) and nonmetal elements (O, N, and S) were located along nanowires, demonstrating that HRP distributes evenly on the PdCu hydrogels (Figure 1e−j).

To further verify the fact that HRP was coated on the surface of hydrogels, a Fourier transform infrared spectrometer was used to characterize PdCu, HRP, and PdCu@HRP. Figure S2a shows clear differences between PdCu and PdCu@HRP, and the characteristic peaks at 3457, 1634, and 1555 cm^{-1} of PdCu@HRP belong to the −NH−, −CONH− (amide I), and amide II of HRP, respectively.[6,14] The confocal laser scanning microscopy images of PdCu hydrogels loaded with RhB-modified HRP are shown in Figure S2c,d. The red fluorescence region in PdCu@HRP-RhB demonstrates the successful immobilization of the enzymes on PdCu hydrogels.[41] XRD patterns in Figure S2b demonstrate that no significant differences are observed after loading HRP on PdCu hydrogels and four characteristic peaks assigned to the face-centered cubic structure are observed.[25,27]

3.2. Performance of Free HRP, PdCu Hydrogel Nanozymes, PdCu + HRP, and PdCu@HRP. To compare the catalytic performances of catalysts before and after immobilizing, the amounts of PdCu and HRP loaded in PdCu@HRP are consistent with the amount of free HRP and bare PdCu hydrogel nanozymes. The loading amounts of HRP were calculated by the standard curve of enzymes (Figure S3).

https://doi.org/10.1021/acsami.1c09100
ACS Appl. Mater. Interfaces 2021, 13, 33383−33391

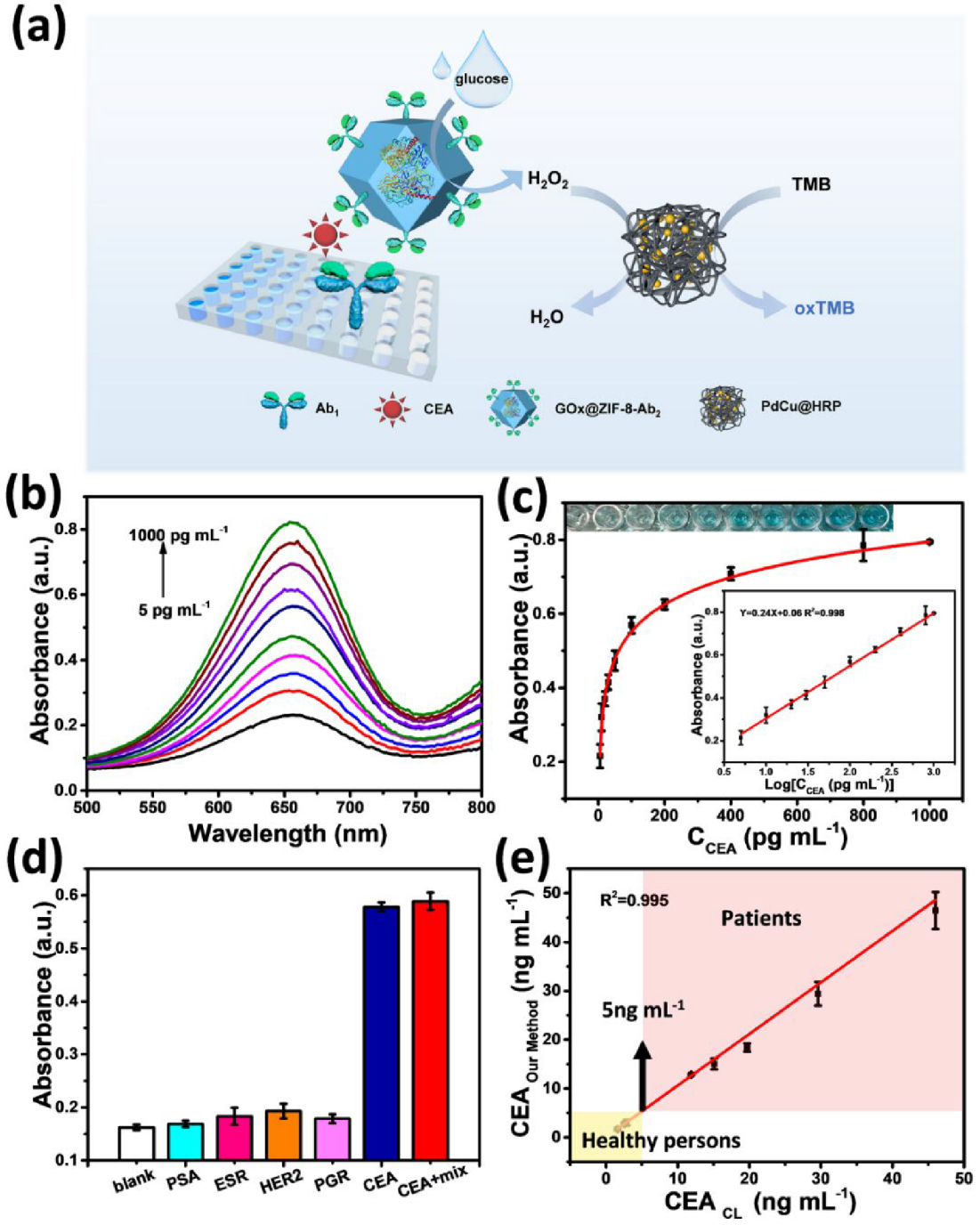

Figure 4. (a) Schematic illustration of the catalytic cascade detection of CEA by ELISA. (b) UV−vis spectra of the detection system with different concentrations of CEA. (c) Corresponding calibration curve. (d) Specificity and selectivity of ELISA (CEA, 100 pg mL^{-1}; PSA, 1 ng mL^{-1}; ESR, 1 ng mL^{-1}; HER2, 1 ng mL^{-1}; PGR, 1 ng mL^{-1}, and the mixture of CEA and interfering antigen). (e) Comparison of the detection concentration obtained from the ELISA by cascade signal amplification and the CL method in the hospital.

TMB can be oxidized to a blue product (oxTMB) by peroxidase with the existence of H_2O_2 (Figure 2a). The catalytic activity of peroxidases can be quantitatively reflected by the absorbance at 652 nm. As shown in Figure 2b, PdCu hydrogels can catalyze the oxidation of TMB with the existence of H_2O_2, indicating that they have peroxidase-like activity. As expected, the color signal of oxTMB catalyzed by the PdCu + HRP system (adding PdCu hydrogel nanozymes and HRP to the substrate solution simultaneously) is stronger than those of free HRP or PdCu hydrogel nanozymes. Significantly, the catalytic activity of PdCu@HRP is the highest among these systems, with an increased absorbance by approximately 1.5-fold than that of the PdCu + HRP system under the same conditions (Figure 2c). It is indicated that not only the peroxidase-like activity of the PdCu hydrogels but also the synergistic effects between the carrier and enzymes play a crucial role in boosting the catalytic activity of PdCu@HRP.

3.3. Stability and Reusability of PdCu Hydrogels, HRP, and PdCu@HRP. Additionally, the tolerance to adverse environments and reusability as keys to practical applications

https://doi.org/10.1021/acsami.1c09100
ACS Appl. Mater. Interfaces 2021, 13, 33383−33391

of PdCu hydrogels, HRP, and PdCu@HRP were investigated. The relative activity of PdCu@HRP, HRP, and PdCu at different pH values and temperatures is shown in Figure 2d,e. Both the optimum pH (4.0) and temperature (37 °C) for PdCu@HRP, HRP, and PdCu hydrogels are the same. The activity of HRP is dramatically reduced when the pH and temperature deviate from the optimal values. However, PdCu@HRP can significantly reduce the loss of enzyme activity with changes in pH and temperature and exhibits higher tolerance in a wider range of pH and temperature, revealing that the porous structure of the hydrogel is favorable for the stability of HRP. The reusability of the PdCu@HRP was also investigated and is plotted in Figure 2. The catalytic activity of PdCu@HRP retained 78.1% of its initial activity after five cycles, while free HRP nearly completely inactivated in the second time, which confirms that enzyme immobilization can facilitate the recovery of enzymes. Such good reusability is attributed to the unique hierarchically porous structure and the high affinity of PdCu hydrogels for HRP, decreasing leakage of the enzymes from carriers to the solution.

3.4. Mechanism of Synergistic Enhancement. To unveil the underlying mechanisms of the enhanced activity of PdCu@HRP, we first explored the interaction between carriers and enzymes. Some common carriers such as ZIF-8, SiO_2, and $Cu_3(PO_4)_2$ were also synthesized and used to load HRP for comparison. The results show that HRP in ZIF-8 and SiO_2 can maintain 94% and 96% activity, respectively (Figure 3 and Table S1). The denaturation and deactivation of the HRP immobilized in ZIF-8 and SiO_2 may be closely associated with mass transfer limitations, unfavorable enzyme−carrier interactions, and conformational changes in the enzymes in the matrix.[4,20,23,24] However, the activity of HRP in $Cu_3(PO_4)_2$ and PdCu hydrogels increases by 1.16- and 2.20-fold in comparison to that of free HRP. The coordination of copper ions in crystals with the imidazole group of histidine in HRP is proposed to trigger the activation of enzymes.[40,42] Furthermore, XPS analysis was performed to explore the electron transfer in the as-obtained PdCu@HRP (Figure 3b,c). Note that the binding energies of the Pd $3d_{5/2}$ and Cu $2p_{3/2}$ peaks of PdCu decrease by 0.9 and 0.6 eV, respectively, after the capsulation of HRP, which demonstrates that PdCu hydrogel nanozymes interact with HRP by coordination interaction and the electrons transferring from HRP to PdCu cause the activation of HRP.

Besides, the interaction between carriers and substrates was explored. Designing suitable supports for immobilizing enzymes is beneficial to capture substrates through hydrophobic or electrostatic interactions.[43,44] As shown in Figure S4, the surface charge of PdCu@HRP is negative after immobilizing positively charged HRP on the negatively charged hydrogel carriers, which is beneficial to attract positively charged substrates by electrostatic interactions.[45,46] To further demonstrate the effect of enrichment of the substrate, the Michaelis−Menten curves of PdCu hydrogel nanozymes, HRP, and PdCu@HRP are plotted in Figure S5. After immobilizing, K_m is reduced by 2.6 and 1.2 times when hydrogen peroxide and TMB are the substrates, respectively (Figure 3d). The detailed kinetic parameters are summarized in Table S2. The surface charge of the catalyst reverses after immobilizing HRP, resulting in a higher substrate concentration near the enzymes than that in the bulk solution, further reducing the Michaelis constant K_m and leading to an apparent increase in enzymatic activity.[20]

3.5. Detection of the CEA Using ELISA by Cascade Signal Amplification. ELISA has been widely explored for the sensing of biomarkers because of the outstanding inherent specificity of immunoreactions.[47−49] The conventional ELISA always uses a HRP-labeled antibody as a signal enhancer, which can oxidize chromophoric molecules and thus realizes the immunoassay of targets. However, the main drawback of the colorimetric method is the relatively low detection sensitivity. Enzyme cascade amplification is a novel and effective signal amplification strategy for improving sensitivity and has been applied for the development of colorimetric immunoassays.[50] In the cascade reaction, an initial enzyme related to a signal receptor is activated and, in turn, catalyzes the activation of numerous secondary enzymes. Here, to achieve signal amplification and ultrasensitive sensing of trace targets, PdCu@HRP-based ELISA was developed through enzyme cascade reactions.[51] To build a new type of cascade biosensor, glucose oxidase (GOx) and PdCu@HRP were combined to realize signal amplification. GOx was encapsulated into ZIF-8 to obtain GOx@ZIF-8. The morphology of the as-prepared GOx@ZIF8-Ab_2 maintains a typical rhombic dodecahedron structure (Figure S6). RhB-labeled GOx was used to prove the successful encapsulation of GOx by CLSM, and a red fluorescence region in the images (Figure S7) was observed, indicating that GOx was encapsulated in ZIF-8. To verify the feasibility of the cascade signal amplification, glucose was added to the GOx@ZIF8 solution and incubated for a while, where H_2O_2 and gluconic acid were produced. The produced H_2O_2 could then effectively oxidize TMB in the presence of PdCu@HRP, and a distinct color change was observed with an increased amount of GOx@ZIF-8, as shown in Figure S8.

The cascade reaction system was employed for the detection of CEA. GOx and the antibody of CEA were integrated into ZIF-8 to form a complex (GOx@ZIF-8-Ab_2) by coprecipitation without any additional chemical coupling reagent (Figure S9). The immunoassay principle is shown in Figure 4a. GOx@ZIF-8-Ab_2 will be recognized by the target CEA, forming sandwich immunocomplexes. Then, PdCu@HRP will be activated in the presence of glucose, resulting in a color change of TMB. Figure 4b shows that the absorbance at 652 nm increased gradually with an increase of CEA concentration, suggesting that a cascade signal amplification system composed of GOx@ZIF-8 and PdCu@HRP can be used for the detection of CEA. A good linear relationship (R^2 = 0.998) in the range of 5−1000 pg mL^{-1} of CEA was established by plotting the absorbance against the logarithm of the CEA concentration (Figure 4c). A limit of detection (LOD) of 1.4 pg mL^{-1} CEA was determined. In comparison, the linear range of 20−800 pg mL^{-1} of CEA with a LOD of 8.5 pg mL^{-1} was determined for the conventional HRP-based ELISA based on its calibration curve (Figure S10). These results suggested that the cascade system could improve the sensitivity by 6.1-fold compared to the conventional HRP-based ELISA. Besides, the resulting sensing platform was compared with other immunoassays utilizing different protocols (Table S3) and showed excellent performances with a low LOD. We also investigated the reproducibility of the developed ELISA by repeatedly measuring 100 pg mL^{-1} CEA five times. As shown in Figure S11, the consistency of the signal intensity indicates satisfactory reproducibility. Besides, the stability was evaluated using the developed method for sensing 100 pg mL^{-1} CEA at different interval days. The signal responses exhibited no

https://doi.org/10.1021/acsami.1c09100
ACS Appl. Mater. Interfaces 2021, 13, 33383−33391

apparent difference in 12 days, demonstrating the good stability of the developed ELISA (Figure S12). Subsequently, the specificity and selectivity of the developed ELISA toward the target CEA and other biomarkers (e.g., prostate-specific antigen, PSA; estrogen receptor, ESR; progesterone receptor, PGR; human epidermal growth factor receptor 2, HER2) were also investigated. As shown in Figure 4d, the interferences including PSA, ESR, HER2, and PGR at a concentration of 1 ng mL^{-1} showed no apparent difference from the blank group. On the contrary, the target CEA with a low concentration (100 pg mL^{-1}) could cause a significant change in the absorbance. Besides, the absorbance intensities did not show significant increases compared with CEA alone when the system contained both the target CEA and interferences. Hence, the PdCu@HRP-based improved ELISA exhibited high specificity and selectivity toward the target CEA.

3.6. Application in Human Serum Samples. To demonstrate the potential application of the PdCu@HRP-based ELISA in clinical diagnosis, the real samples of human serum from healthy people and patients were analyzed. The CEA levels of human serum obtained from the hospital are in the range of 1.62−46 ng mL^{-1}, which are outside of the linear range. Hence, the human serum was diluted 100 times with PBS solution before the immunoassay. The comparison between the detected value obtained by the proposed ELISA and the testing value from the hospital (chemiluminescence (CL) method) shows a good linear relationship and R^2 equals 0.995, indicating that the proposed strategy could be utilized as an optional scheme for the quantitative determination of target CEA in practical applications (Figure 4e).

4. CONCLUSIONS

In this work, we have successfully developed PdCu hydrogel nanozymes to immobilize HRP, which can enhance the thermal and chemical stabilities of HRP, realizing the reuse of enzymes. Significantly, PdCu@HRP exhibits synergistically enhanced peroxidase activity than the free HRP and PdCu hydrogel nanozymes, demonstrating the unique advantages of the noble metal hydrogels as support for immobilizing enzymes. Accordingly, the resulting PdCu@HRP was applied in ELISA to detect CEA by a cascade reaction for signal amplification. The proposed biosensor realizes the quantitative probing of the CEA concentration in a wide range from 5 to 1000 pg mL^{-1} with a LOD of 1.4 pg mL^{-1}, exhibiting 6.1-fold enhanced sensitivity than HRP-based ELISA. This work broadens the application of noble metal hydrogels and provides a new view for immobilizing enzymes.

■ ASSOCIATED CONTENT

Supporting Information

The Supporting Information is available free of charge at https://pubs.acs.org/doi/10.1021/acsami.1c09100.

Materials and instruments; synthesis of GOx@ZIF-8, GOx@ZIF-8-Ab_2, HRP@ZIF-8, SiO_2-HRP, and $Cu_3(PO_4)_2$-HRP; digital photos and SEM, TEM, and HRTEM images; FT-IR spectra, XRD patterns, and CLSM images; standard curve of HRP concentration; ζ potentials; kinetic curves and comparisons of kinetic parameters; comparison of the HRP-support systems with enzyme activities; absorption spectra for feasibility; scheme of the preparation of GOx@ZIF-8-Ab_2; linear calibration of HRP-based ELISA; reproducibility and stability of developed ELISA; and comparison with other methods (PDF)

■ AUTHOR INFORMATION

Corresponding Author

Chengzhou Zhu − *Key Laboratory of Pesticide and Chemical Biology of Ministry of Education, International Joint Research Center for Intelligent Biosensing Technology and Health, College of Chemistry, Central China Normal University, Wuhan 430079, P. R. China;* orcid.org/0000-0003-0679-7965; Email: czzhu@mail.ccnu.edu.cn

Authors

Jiajia Huang − *Key Laboratory of Pesticide and Chemical Biology of Ministry of Education, International Joint Research Center for Intelligent Biosensing Technology and Health, College of Chemistry, Central China Normal University, Wuhan 430079, P. R. China*

Lei Jiao − *Key Laboratory of Pesticide and Chemical Biology of Ministry of Education, International Joint Research Center for Intelligent Biosensing Technology and Health, College of Chemistry, Central China Normal University, Wuhan 430079, P. R. China*

Weiqing Xu − *Key Laboratory of Pesticide and Chemical Biology of Ministry of Education, International Joint Research Center for Intelligent Biosensing Technology and Health, College of Chemistry, Central China Normal University, Wuhan 430079, P. R. China*

Qie Fang − *Key Laboratory of Pesticide and Chemical Biology of Ministry of Education, International Joint Research Center for Intelligent Biosensing Technology and Health, College of Chemistry, Central China Normal University, Wuhan 430079, P. R. China*

Hengjia Wang − *Key Laboratory of Pesticide and Chemical Biology of Ministry of Education, International Joint Research Center for Intelligent Biosensing Technology and Health, College of Chemistry, Central China Normal University, Wuhan 430079, P. R. China*

Xiaoli Cai − *Key Laboratory of Pesticide and Chemical Biology of Ministry of Education, International Joint Research Center for Intelligent Biosensing Technology and Health, College of Chemistry, Central China Normal University, Wuhan 430079, P. R. China*

Hongye Yan − *Key Laboratory of Pesticide and Chemical Biology of Ministry of Education, International Joint Research Center for Intelligent Biosensing Technology and Health, College of Chemistry, Central China Normal University, Wuhan 430079, P. R. China*

Wenling Gu − *Key Laboratory of Pesticide and Chemical Biology of Ministry of Education, International Joint Research Center for Intelligent Biosensing Technology and Health, College of Chemistry, Central China Normal University, Wuhan 430079, P. R. China*

Complete contact information is available at: https://pubs.acs.org/10.1021/acsami.1c09100

Author Contributions

#J.H. and L.J. contributed equally to this work. All authors have approved the final version of the manuscript.

Notes

The authors declare no competing financial interest.

■ ACKNOWLEDGMENTS

The authors gratefully acknowledge the financial support by the National Natural Science Foundation of China (nos. 22074049 and 22004042), the Fundamental Research Funds for the Central Universities (nos. CCNU20QN007 and CCNU20TS013), and the Program of Introducing Talents of Discipline to Universities of China (111 Program, B17019).

■ REFERENCES

(1) Zhou, Z.; Hartmann, M. Progress in Enzyme Immobilization in Ordered Mesoporous Materials and Related Applications. *Chem. Soc. Rev.* **2013**, *42*, 3894−3912.
(2) Wu, J.; Wang, X.; Wang, Q.; Lou, Z.; Li, S.; Zhu, Y.; Qin, L.; Wei, H. Nanomaterials with Enzyme-like Characteristics (Nanozymes): Next-Generation Artificial Enzymes (II). *Chem. Soc. Rev.* **2019**, *48*, 1004−1076.
(3) Wang, Q.; Wei, H.; Zhang, Z.; Wang, E.; Dong, S. Nanozyme: An Emerging Alternative to Natural Enzyme for Biosensing and Immunoassay. *TrAC, Trends Anal. Chem.* **2018**, *105*, 218−224.
(4) Lian, X.; Fang, Y.; Joseph, E.; Wang, Q.; Li, J.; Banerjee, S.; Lollar, C.; Wang, X.; Zhou, H. C. Enzyme-MOF (Metal-Organic Framework) Composites. *Chem. Soc. Rev.* **2017**, *46*, 3386−3401.
(5) Pina, D. G.; Shnyrova, A. V.; Gavilanes, F.; Rodríguez, A.; Leal, F.; Roig, M. G.; Sakharov, I. Y.; Zhadan, G. G.; Villar, E.; Shnyrov, V. L. Thermally Induced Conformational Changes in Horseradish Peroxidase. *Eur. J. Biochem.* **2001**, *268*, 120−126.
(6) Monier, M.; Ayad, D. M.; Wei, Y.; Sarhan, A. A. Immobilization of Horseradish Peroxidase on Modified Chitosan Beads. *Int. J. Biol. Macromol.* **2010**, *46*, 324−330.
(7) Jiao, L.; Yan, H.; Wu, Y.; Gu, W.; Zhu, C.; Du, D.; Lin, Y. When Nanozymes Meet Single-Atom Catalysis. *Angew. Chem., Int. Ed.* **2020**, *59*, 2565−2576.
(8) Bian, J.; An, X.; Jiang, W.; Liu, R.; Hu, C.; Liu, H. Defect-Enhanced Activation of Carbon Nitride/Horseradish Peroxidase Nanohybrids for Visible-Light-Driven Photobiocatalytic Water Purification. *Chem. Eng. J.* **2021**, *408*, No. 127231.
(9) Zhai, R.; Zhang, B.; Wan, Y.; Li, C.; Wang, J.; Liu, J. Chitosan-Halloysite Hybrid-Nanotubes: Horseradish Peroxidase Immobilization and Applications in Phenol Removal. *Chem. Eng. J.* **2013**, *214*, 304−309.
(10) Huang, J.; Sommers, E. M.; Kim-Shapiro, D. B.; King, S. B. Horseradish Peroxidase Catalyzed Nitric Oxide Formation from Hydroxyurea. *J. Am. Chem. Soc.* **2002**, *124*, 3473−3480.
(11) Gong, C.; Gong, Y.; Khaing Oo, M. K.; Wu, Y.; Rao, Y.; Tan, X.; Fan, X. Sensitive Sulfide Ion Detection by Optofluidic Catalytic Laser Using Horseradish Peroxidase (HRP) Enzyme. *Biosens. Bioelectron.* **2017**, *96*, 351−357.
(12) Yang, Y.; Zhao, M.; Yao, P.; Huang, Y.; Dai, Z.; Yuan, H.; Ni, C. Comparative Studies on Enzyme Activity of Immobilized Horseradish Peroxidase in Silica Nanomaterials with Three Different Shapes and Methoxychlor Degradation of Vesicle-Like Mesoporous SiO_2 as Carrier. *J. Nanosci. Nanotechnol.* **2018**, *18*, 2971−2978.
(13) Chen, G.; Kou, X.; Huang, S.; Tong, L.; Shen, Y.; Zhu, W.; Zhu, F.; Ouyang, G. Modulating the Biofunctionality of Metal-Organic-Framework-Encapsulated Enzymes through Controllable Embedding Patterns. *Angew. Chem., Int. Ed.* **2020**, *59*, 2867−2874.
(14) Xiao, F.; Xiao, P.; Jiang, W.; Wang, D. Immobilization of Horseradish Peroxidase on Fe_3O_4 Nanoparticles for Enzymatic Removal of Endocrine Disrupting Chemicals. *Environ. Sci. Pollut. Res. Int.* **2020**, *27*, 24357−24368.
(15) Rubtsova, M. Y.; Kovba, G. V.; Egorov, A. M. Chemiluminescent Biosensors Based on Porous Supports with Immobilized Peroxidase. *Biosens. Bioelectron.* **1998**, *13*, 75−85.
(16) Liu, H.; Guo, K.; Lv, J.; Gao, Y.; Duan, C.; Deng, L.; Zhu, Z. A Novel Nitrite Biosensor Based on the Direct Electrochemistry of Horseradish Peroxidase Immobilized on Porous Co_3O_4 Nanosheets and Reduced Graphene Oxide Composite Modified Electrode. *Sens. Actuators, B* **2017**, *238*, 249−256.
(17) Lv, S.; Zhang, K.; Zhu, L.; Tang, D.; Niessner, R.; Knopp, D. H_2-Based Electrochemical Biosensor with Pd Nanowires@ZIF-67 Molecular Sieve Bilayered Sensing Interface for Immunoassay. *Anal. Chem.* **2019**, *91*, 12055−12062.
(18) Lv, S.; Zhang, K.; Zhu, L.; Tang, D. ZIF-8-Assisted NaYF4: Yb, Tm@ZnO Converter with Exonuclease III-Powered DNA Walker for Near-Infrared Light Responsive Biosensor. *Anal. Chem.* **2020**, *92*, 1470−1476.
(19) Li, P.; Modica, J. A.; Howarth, A. J.; Vargas, L.; Moghadam, E.; Peyman, Z.; Snurr, R. Q.; Mrksich, M.; Hupp, J. T.; Farha, O. K. Toward Design Rules for Enzyme Immobilization in Hierarchical Mesoporous Metal-Organic Frameworks. *Chem.* **2016**, *1*, 154−169.
(20) Zhang, Y.; Ge, J.; Liu, Z. Enhanced Activity of Immobilized or Chemically Modified Enzymes. *ACS Catal.* **2015**, *5*, 4503−4513.
(21) Rodrigues, R. C.; Ortiz, C.; Berenguer-Murcia, A.; Torres, R.; Fernandez-Lafuente, R. Modifying Enzyme Activity and Selectivity by Immobilization. *Chem. Soc. Rev.* **2013**, *42*, 6290−6307.
(22) Sheldon, R. A.; Van Pelt, S. Enzyme Immobilisation in Biocatalysis: Why, What and How. *Chem. Soc. Rev.* **2013**, *42*, 6223−6235.
(23) Liang, J.; Gao, S.; Liu, J.; Zulkifli, M. Y.; Xu, J.; Scott, J.; Chen, V.; Shi, J.; Rawal, A.; Liang, K. Hierarchically Porous Biocatalytic MOF Microreactor as a Versatile Platform towards Enhanced Multienzyme and Cofactor-Dependent Biocatalysis. *Angew. Chem., Int. Ed.* **2021**, *60*, 5421−5428.
(24) Li, G.; Ma, P.; He, Y.; Zhang, Y.; Luo, Y.; Zhang, C.; Fan, H. Enzyme-Nanowire Mesocrystal Hybrid Materials with an Extremely High Biocatalytic Activity. *Nano Lett.* **2018**, *18*, 5919−5926.
(25) Zhu, C.; Shi, Q.; Fu, S.; Song, J.; Xia, H.; Du, D.; Lin, Y. Efficient Synthesis of MCu (M = Pd, Pt, and Au) Aerogels with Accelerated Gelation Kinetics and Their High Electrocatalytic Activity. *Adv. Mater.* **2016**, *28*, 8779−8783.
(26) Wu, Y.; Jiao, L.; Xu, W.; Gu, W.; Zhu, C.; Du, D.; Lin, Y. Polydopamine-Capped Bimetallic AuPt Hydrogels Enable Robust Biosensor for Organophosphorus Pesticide Detection. *Small* **2019**, *15*, No. 1900632.
(27) Wang, H.; Zhang, S.; Cai, W.; Xu, B. Z.; Cai, Z.; Wu, Y.; Luo, X.; Wei, X.; Liu, Z.; Gu, W.; Eychmüller, A.; Zhu, C.; Chen, J. Largely Boosted Methanol Electrooxidation Using Ionic Liquid/PdCu Aerogels via Interface Engineering. *Mater. Horiz.* **2020**, *7*, 2407−2413.
(28) Zhu, C.; Du, D.; Eychmuller, A.; Lin, Y. Engineering Ordered and Nonordered Porous Noble Metal Nanostructures: Synthesis, Assembly, and Their Applications in Electrochemistry. *Chem. Rev.* **2015**, *115*, 8896−8943.
(29) Liu, W.; Herrmann, A. K.; Bigall, N. C.; Rodriguez, P.; Wen, D.; Oezaslan, M.; Schmidt, T. J.; Gaponik, N.; Eychmuller, A. Noble Metal Aerogels-Synthesis, Characterization, and Application as Electrocatalysts. *Acc. Chem. Res.* **2015**, *48*, 154−162.
(30) Fan, X.; Zerebecki, S.; Du, R.; Hübner, R.; Marzum, G.; Jiang, G.; Hu, Y.; Barcikowki, S.; Reichenberger, S.; Eychmüller, A. Promoting the Electrocatalytic Performance of Noble Metal Aerogels by Ligand-Directed Modulation. *Angew. Chem., Int. Ed.* **2020**, *59*, 5706−5711.
(31) Du, R.; Joswig, J.-O.; Hübner, R.; Zhou, L.; Wei, W.; Hu, Y.; Eychmüller, A. Back Cover: Freeze-Thaw-Promoted Fabrication of Clean and Hierarchically Structured Noble-Metal Aerogels for Electrocatalysis and Photoelectrocatalysis. *Angew. Chem., Int. Ed.* **2020**, *59*, 8302−8302.
(32) Jiao, L.; Xu, W.; Yan, H.; Wu, Y.; Gu, W.; Li, H.; Du, D.; Lin, Y.; Zhu, C. A Dopamine-Induced Au Hydrogel Nanozyme for Enhanced Biomimetic Catalysis. *Chem. Commun.* **2019**, *55*, 9865−9868.
(33) Wang, H.; Fang, Q.; Gu, W.; Du, D.; Lin, Y.; Zhu, C. Noble Metal Aerogels. *ACS Appl. Mater. Interfaces* **2020**, *12*, 52234−52250.
(34) Maruyama, T.; Terashima, Y.; Takeda, S.; Okazaki, F.; Goto, M. Selective Adsorption and Recovery of Precious Metal Ions Using Protein-Rich Biomass as Efficient Adsorbents. *Process Biochem.* **2014**, *49*, 850−857.

https://doi.org/10.1021/acsami.1c09100
ACS Appl. Mater. Interfaces 2021, 13, 33383−33391

(35) Alhazmi, H. A.; Nachbar, M.; Albishri, H. M.; Abd El-Hady, D.; Redweik, S.; El Deeb, S.; Watzig, H. A Comprehensive Platform to Investigate Protein-Metal Ion Interactions by Affinity Capillary Electrophoresis. *J. Pharm. Biomed. Anal.* **2015**, *107*, 311−317.
(36) Kiyoyama, S.; Maruyama, T.; Kamiya, N.; Goto, M. Immobilization of Proteins into Microcapsules and Their Adsorption Properties with Respect to Precious-Metal Ions. *Ind. Eng. Chem. Res.* **2008**, *47*, 1527−1532.
(37) Shen, X.; Liu, W.; Gao, X.; Lu, Z.; Wu, X.; Gao, X. Mechanisms of Oxidase and Superoxide Dismutation-Like Activities of Gold, Silver, Platinum, and Palladium, and Their Alloys: A General Way to the Activation of Molecular Oxygen. *J. Am. Chem. Soc.* **2015**, *137*, 15882−15891.
(38) Yu, Z.; Cai, G.; Liu, X.; Tang, D. Platinum Nanozyme-Triggered Pressure-Based Immunoassay Using a Three-Dimensional Polypyrrole Foam-Based Flexible Pressure Sensor. *ACS Appl. Mater. Interfaces* **2020**, *12*, 40133−40140.
(39) Huang, L.; Yu, Z.; Chen, J.; Tang, D. Pressure-Based Bioassay Perceived by a Flexible Pressure Sensor with Synergistic Enhancement of the Photothermal Effect. *ACS Appl. Bio Mater.* **2020**, *3*, 9156−9163.
(40) Arnold, F. H. Metal-Affinity Separations: A New Dimension in Protein Processing. *Nat. Biotechnol.* **1991**, *9*, 151−156.
(41) Xu, W.; Jiao, L.; Yan, H.; Wu, Y.; Chen, L.; Gu, W.; Du, D.; Lin, Y.; Zhu, C. Glucose Oxidase-Integrated Metal-Organic Framework Hybrids as Biomimetic Cascade Nanozymes for Ultrasensitive Glucose Biosensing. *ACS Appl. Mater. Interfaces* **2019**, *11*, 22096−22101.
(42) Lin, Z.; Xiao, Y.; Yin, Y.; Hu, W.; Liu, W.; Yang, H. Facile Synthesis of Enzyme-Inorganic Hybrid Nanoflowers and Its Application as a Colorimetric Platform for Visual Detection of Hydrogen Peroxide and Phenol. *ACS Appl. Mater. Interfaces* **2014**, *6*, 10775−10782.
(43) Cheng, K.; Svec, F.; Lv, Y.; Tan, T. Hierarchical Micro- and Mesoporous Zn-Based Metal-Organic Frameworks Templated by Hydrogels: Their Use for Enzyme Immobilization and Catalysis of Knoevenagel Reaction. *Small* **2019**, *15*, No. 1902927.
(44) Lyu, F.; Zhang, Y.; Zare, R. N.; Ge, J.; Liu, Z. One-Pot Synthesis of Protein-Embedded Metal-Organic Frameworks with Enhanced Biological Activities. *Nano Lett.* **2014**, *14*, 5761−5765.
(45) Liu, S.; Huang, B.; Zheng, G.; Zhang, P.; Li, J.; Yang, B.; Chen, Y. P.; Liang, L. Nanocapsulation of Horseradish Peroxidase (HRP) Enhances Enzymatic Performance in Removing Phenolic Compounds. *Int. J. Biol. Macromol.* **2020**, *150*, 814−822.
(46) Besharati Vineh, M.; Saboury, A. A.; Poostchi, A. A.; Rashidi, A. M.; Parivar, K. Stability and Activity Improvement of Horseradish Peroxidase by Covalent Immobilization on Functionalized Reduced Graphene Oxide and Biodegradation of High Phenol Concentration. *Int. J. Biol. Macromol.* **2018**, *106*, 1314−1322.
(47) Jin, L. Y.; Dong, Y. M.; Wu, X. M.; Cao, G. X.; Wang, G. L. Versatile and Amplified Biosensing through Enzymatic Cascade Reaction by Coupling Alkaline Phosphatase in Situ Generation of Photoresponsive Nanozyme. *Anal. Chem.* **2015**, *87*, 10429−10436.
(48) Ruan, X.; Liu, D.; Niu, X.; Wang, Y.; Simpson, C. D.; Cheng, N.; Du, D.; Lin, Y. 2D Graphene Oxide/Fe-MOF Nanozyme Nest with Superior Peroxidase-Like Activity and Its Application for Detection of Woodsmoke Exposure Biomarker. *Anal. Chem.* **2019**, *91*, 13847−13854.
(49) Jiao, L.; Yan, H.; Xu, W.; Wu, Y.; Gu, W.; Li, H.; Du, D.; Lin, Y.; Zhu, C. Self-Assembly of All-Inclusive Allochroic Nanoparticles for the Improved ELISA. *Anal. Chem.* **2019**, *91*, 8461−8465.
(50) Li, J.; Gao, Z.; Ye, H.; Wan, S.; Pierce, M.; Tang, D.; Xia, X. A Non-enzyme Cascade Amplification Strategy for Colorimetric Assay of Disease Biomarkers. *Chem. Commun.* **2017**, *53*, 9055−9058.
(51) Hwang, E. T.; Lee, S. Multienzymatic Cascade Reactions via Enzyme Complex by Immobilization. *ACS Catal.* **2019**, *9*, 4402−4425.

https://doi.org/10.1021/acsami.1c09100
ACS Appl. Mater. Interfaces 2021, 13, 33383−33391